Dalton Transactions

PAPER

View Article Online
View Journal | View Issue

CrossMark click for updates

Cite this: *Dalton Trans.*, 2016, **45**, 6149

Group 13 metal complexes containing the bis-(4-methylbenzoxazol-2-yl)-methanide ligand†‡

David-R. Dauer, Melchior Flügge, Regine Herbst-Irmer and Dietmar Stalke*

Received 6th October 2015,
Accepted 19th November 2015

DOI: 10.1039/c5dt03913d

www.rsc.org/dalton

To focus on the high importance of low-valent main group metal complexes, which can be applied to catalytic transformations, this article deals with the promising new ligand system (4-MeNCOC$_6$H$_3$)$_2$CH$_2$ (**1**). It is patterned on the well known nacnac ligand and further development of the parent bisheterocyclo methanes. In comparison with the results of previous studies based on the bisheterocyclo methanes (NCOC$_6$H$_4$)$_2$CH$_2$ and (NCOC$_6$H$_4$)$_2$CH$_2$ derivative **1** was modified by adding a methyl group to the annulated benzene perimeters to enhance the steric protection of a potentially coordinated main group metal cation. On reaction of **1** with group 13 trimethyl reagents and dialkyl aluminium halides the ligand backbone gets deprotonated and the two endocyclic nitrogen donor atoms coordinate with the remaining organometallic fragment to form a six-membered metalla heterocycle. The synthesis of [Me$_2$Al{(4-MeNCOC$_6$H$_3$)$_2$CH}] (**2**), [Me$_2$Ga{(4-MeNCOC$_6$H$_3$)$_2$CH}] (**3**), [Me$_2$In{(4-MeNCOC$_6$H$_3$)$_2$CH}] (**4**), [ClMeAl{(4-MeNCOC$_6$H$_3$)$_2$CH}] (**5**), [IMeAl{(4-MeNCOC$_6$H$_3$)$_2$CH}] (**6**) and [IEtAl{(4-MeNCOC$_6$H$_3$)$_2$CH}] (**7**) could be accomplished. A structural comparison of those metallated species based on single crystal X-ray analyses identifies them as ideal precursors generating new low-valent main group complexes.

Introduction

In the context of the ongoing increasing demand for the activation of small molecules like H_2, N_2, NH_3 or CO_2 the development of new synthetic approaches for generating catalytic active species is of high interest. Even though this research area of catalytic activation is mostly focused on the field of transition metal complexes the transfer to suitable main group metal complexes, which should adopt the same catalytic reactivity compared to the transition metals or even exceed them, plays a key role in current research.[1]

As a figurehead for efficient small molecule activation FLP (frustrated Lewis pairs) chemistry has developed to a promising research area over the last decade.[2] In this way the usage of mainly phosphorus/boron, nitrogen/boron or carbon/boron FLP systems offers simple access to the efficient splitting of dihydrogen[3] or the ring opening of THF.[4] Also the aluminium based FLPs were found to be advantageous for B–H or N–H bond activation,[5] polymerisation reaction of methyl methacrylate[6] and conversion of CO_2.[7] Furthermore, the well-known nacnac ligand and the derived main group metal complexes, respectively, facilitate the stabilisation of metal ions in low oxidation states.[8] The synthesis of the first Mg(I) compound[9] and the corresponding β-diketiminate Ca(II) complexes,[10] which were successfully applied for epoxide/CO_2 copolymerisation[11] or hydrogenation reactions of alkenes with H_2,[12] should be highlighted as alkaline earth metal complexes performing in catalysis. Switching to group 13 elements also a variety of Al(III) and Ga(III) containing complexes was synthesised and fully characterized.[13] Subsequently also the low-valent Al(I)[14] and Ga(I)[15] species employing the Dipp-substituted (Dipp = 2,6-diisopropylphenyl) nacnac ligand were accessible. More recently the catalytic activity of the related alumoxanes was studied in detail.[16] Other common ligand types, which are used for stabilisation of dimeric low-valent group 13 species involving metal–metal multiple bonds, are the substituted terphenyls, which are also prone to interaction with small molecules like H_2.[17]

With this in mind in the field of main group transformation ligand design in particular and the choice of the suitable main group element have significant influence on the stability and the catalytic abilities of the resulting compounds. In this work we tried to mimic the omnipresent nacnac ligand by two methylene bridged substituted benzoxazole moieties. The corresponding group 13 metal complexes were synthesised to get the best from two worlds: the stabilisation abilities to get low-valent metal complexes and the reactivity of group

Institut für Anorganische Chemie, Georg-August-Universität Göttingen, Tammannstraße 4, 37077 Göttingen, Germany.
E-mail: dstalke@chemie.uni-goettingen.de

† Dedicated to Prof. Herbert W. Roesky on the occasion of his 80th birthday.

‡ Electronic supplementary information (ESI) available: Tables of data collection parameters, bond lengths and angles of compounds **1–7** and further information for side product **1a**. CCDC 1429338, 1429339, 1429341–1429343, 1429357, and 1429403. For ESI and crystallographic data in CIF or other electronic format see DOI: 10.1039/c5dt03913d

13 metals. To tie up with earlier studies concerning the related bisheterocyclo methanide[18] and amide derivatives[19] this work focuses on bis-(4-methylbenzoxazol-2-yl)-methane **1**. The previous results of the methanide containing metal complexes have shown that upon deprotonation of the methylene bridge of the parent ligand systems the coordination of the metal cation is preferentially accomplished by the endocyclic nitrogen donor atoms in a chelating fashion.[20] Due to this fact and to further shield the coordinated metal the bis-(benzoxazol-2-yl)-methane ligand was additionally methyl substituted in **1** to increase the kinetic stabilisation at the same side of the coordinating nitrogen atoms. Neither in the case of the methanide nor the amide derivatives a coordination *via* the other feasible O- or S-coordinating sites has been observed in the solid state yet.[18,19]

The issue of steric shielding of metal centres within the group 13 complexes is an important aspect for further applications and reactions, because in the future we plan to convert these Al(III) containing species into the low-valent Al(I) compounds *e.g.* [Al{Dipp$_2$nacnac}].[14e] Because of the high electrophilicity of the Al(I) species steric protection is essential to maintain the monomeric carbene-like structural motif and prevent dimerisation or nucleophilic attacks.[21] The challenge to synthesise a low-valent species containing a bisheterocyclo methanide ligand backbone is still the guiding idea of ongoing research and **1** seems to be a promising ligand system for the subsequent reduction steps (*vide infra*).

Among the nacnac derivatives and the bisheterocyclo methanides efficient metal shielding is comparable within certain limits. In the case of the nacnac ligands the residues at the bulky imine moieties are twisted nearly perpendicularly with respect to the chelating C_3N_2M-plane, which causes the metal atoms to be most protected. In the case of the complexes derived from **1** the methyl groups shield as well but due to less steric congestion the metal centres are slightly more accessible for allowing some specific substitution reactions. The new metal complexes containing a central six-membered metalla heterocycle are reminiscent of the analogous metal complexes with the omnipresent nacnac ligand. The following similarities between the herein discussed bisheterocyclo methanides and the nacnac ligands can be stated due to the structural comparison of the corresponding metal complexes: Firstly the deprotonation of the bridging moiety leads to the formation of a negative charge in the ligand's backbone, which is completely delocalised to give 6π electrons containing the metalla heterocycle (see Table 1). Secondly, the chelating coordination of the metal cation is achieved exclusively by the two nitrogen donor atoms in the ligand periphery.

Table 1 Selected averaged bond lengths (Å) and angles (°) of the ligand backbone for compounds **1–4** and reference structures

	C_{ipso}–C1′	C_{ipso}–N	C1–C1′–C8
(4-MeNCOC$_6$H$_4$)$_2$CH$_2$ (**1**)	1.487(2)	1.291(2)	110.79(12)
[Me$_2$Al{(4-MeNCOC$_6$H$_4$)$_2$CH}] (**2**)	1.384(2)	1.351(2)	121.13(14)
[Me$_2$Ga{(4-MeNCOC$_6$H$_4$)$_2$CH}] (**3**)	1.388(3)	1.341(2)	121.62(18)
[Me$_2$In{(4-MeNCOC$_6$H$_4$)$_2$CH}] (**4**)	1.390(13)	1.337(12)	123.6(6)
[Me$_2$Al{(NCOC$_6$H$_4$)$_2$CH}][18]	1.380(3)	1.346(3)	119.5(2)
[Me$_2$Al{(NCSC$_6$H$_4$)$_2$CH}][18]	1.390(2)	1.352(2)	123.54(14)
[Me$_2$Al{(NCSC$_6$H$_4$)$_2$N}][19]	—	1.331(3)	—
[Me$_2$Al{(4-MeNCSC$_6$H$_4$)$_2$N}][19]	—	1.343(2)	—

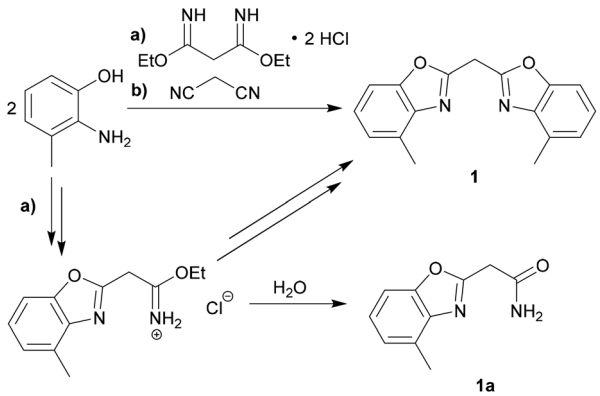

Scheme 1 Synthetic routes to the parent ligand system **1** including the side product **1a**.

Results and discussion

Ligand synthesis

The synthesis of the parent uncharged ligand system is achieved as reported earlier for the corresponding unsubstituted bis-(benzoxazol-2-yl)- and bis-(benzothiazol-2-yl)-methanes.[18,22] A cyclocondensation reaction of two equivalents of 2-amino-3-methylphenol and one equivalent of a C_3-linker unit derived from malonic acid yields the ligand. Two different synthesis routes were performed and optimised to give a moderate overall yield of 56% (see Scheme 1).

The first route is through the synthesis of the unsubstituted bis-(benzoxazol-2-yl)-methane, in which a bisimidate linker was used for the coupling of the two phenol derivatives. This pathway, however, leads to a smaller yield of the desired product **1** and also promotes the formation of a specific side product **1a**. The side product could be identified as 4-methylbenzoxazol-2-yl-carboxamide, which occurs, if just one equivalent of the starting material has cyclised and the remaining imidate unit has been hydrolysed upon further purification. On the second improved route malonic dinitrile was added to the phenolic starting material. In that case polyphosphoric acid (ppa) was added as a solvent and catalytically facilitates the cyclisation reaction to give the parent ligand system **1**.

Compound **1** crystallises in the triclinic space group $P\bar{1}$ and the asymmetric unit contains one molecule (Fig. 1). Like the other symmetrically substituted bisheterocyclo methanes[18] the central carbon atom C1′ is also coordinated in a distorted tetrahedral fashion and the benzoxazole moieties are twisted nearly perpendicularly (81.53(4)°) relative to each other. Due to

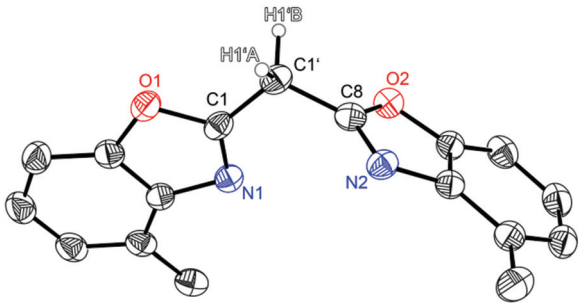

Fig. 1 Molecular structure of $(4\text{-MeNCOC}_6H_3)_2CH_2$ (**1**). Anisotropic displacement parameters are depicted at the 50% probability level. C–H hydrogen atoms are omitted for clarity except for the bridging ones. Structural data are given in Tables 1–3.

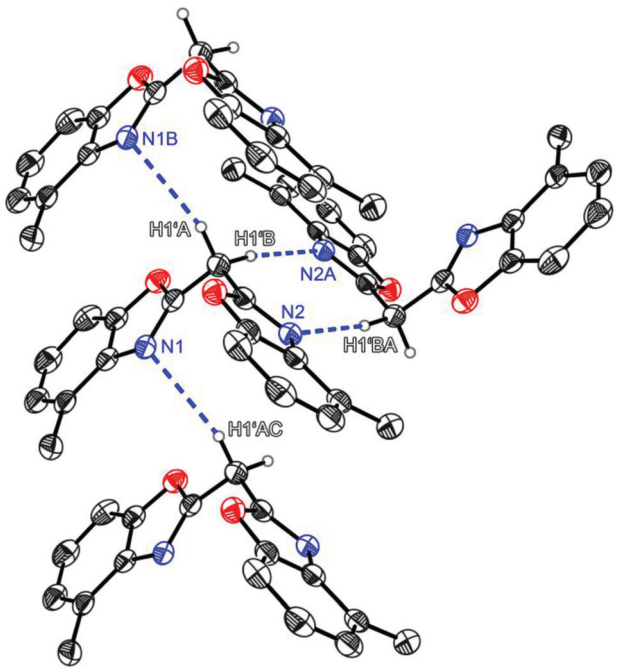

Fig. 2 Hydrogen bonding properties of the parent ligand system $(4\text{-MeNCOC}_6H_3)_2CH_2$ (**1**).

the higher steric demand of the heterocycles the C1–C1′–C8 angle is widened to 110.8(1)°, whereas all other angles around C1′ are slightly compressed in comparison with an ideal tetrahedral angle. Interestingly in the solid state **1** forms a 3D network of quite remarkable C–H···N hydrogen bonds, in which the two acidic methylene hydrogen atoms of the bridge are coordinated by imine nitrogen atoms of two adjacent molecules (see Fig. 2). The experimentally determined values show two hydrogen bonds each, which are energetically more favourable (H1′B···N2: 2.39 Å; C1′–H1′B···N2: 171.1°), and two which are less pronounced (H1′A···N1: 2.62 Å; C1′–H1′A···N1: 150.9°).

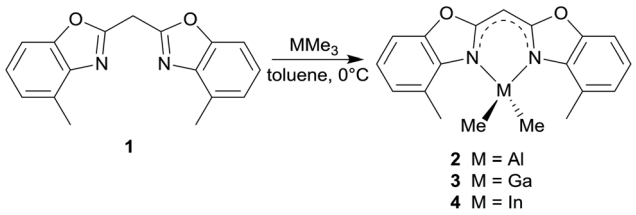

Scheme 2 Metallation reactions of **1**.

Syntheses of the group 13 metal complexes

The reaction of **1** in toluene with pure trimethyl aluminium, gallium or indium leads to the formation of the monoanionic methanides containing the corresponding MMe_2 fragment (see Scheme 2). By the addition of these organometallic reagents the acidic methylene bridge gets deprotonated with the evolution of gaseous methane and in a concerted manner the remaining dimethyl group 13 metal cation gets chelated by the two ring nitrogen donor atoms.

Upon deprotonation the concerned C_{ipso}–C_{bridge} distances are shortened in comparison with **1** and the C_{ipso}–N distances are slightly elongated (Table 1). This is caused by two facts, which are important for structural features. On the one hand the deprotonation of the central methylene moiety generates a free electron pair. Because of the adjacent conjugated π-systems of the two benzoxazole units this free electron pair tends to be delocalised over the whole ligand framework resulting in different feasible resonance structures: carbanionic, amidic or completely delocalised. On the other hand the hybridisation of the central carbon atom changes from sp^3 in the starting material **1** to sp^2 in the metallated species **2–4** based on the trigonal planar coordination geometry of C1′.

Structural comparison of 2–4

A closer look at the experimentally determined geometry of **1** shows that the C_{ipso}–C_{bridge} distance is slightly shorter than what is to be expected for a typical $C(sp^2)$–$C(sp^3)$ single bond (1.51 Å). This deviation can be explained by the presence of the four electronegative adjacent heteroatoms, which cause the C_{ipso}–C_{bridge} bonds to shrink due to their electron withdrawing ability.

In comparison with compounds **2–4** the observed C_{ipso}–C_{bridge} distances (1.384 Å to 1.390 Å) are half way between a typical $C(sp^2)$–$C(sp^2)$ single bond (1.47 Å) and a $C(sp^2)$=$C(sp^2)$ double bond (1.34 Å), which is a result of the efficient delocalisation of the double bonds. The same explanation is valid for the C_{ipso}–N bond lengths, which are in a narrow range from 1.337 Å to 1.351 Å. These values for the C_{ipso}–N bond lengths can also be seen as the average of a typical $C(sp^2)$–$N(sp^2)$ single bond (1.40 Å) and a $C(sp^2)$=$N(sp^2)$ double bond (1.29 Å).[23] In light of the previous results of the methanides $[Me_2Al\{(NCOC_6H_4)_2CH\}]$ and $[Me_2Al\{(NCSC_6H_4)_2CH\}]$[18] and the analogous amide bridged species $[Me_2Al\{(NCSC_6H_4)_2N\}]$ and $[Me_2Al\{(4\text{-MeNCSC}_6H_4)_2N\}]$[19] the discussed structural values match well (Table 1).

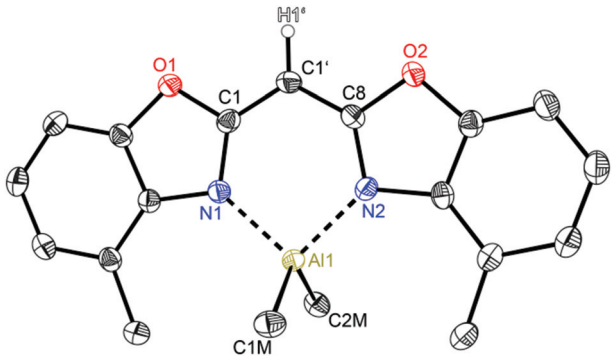

Fig. 3 Molecular structure of $[Me_2Al\{(4\text{-}MeNCOC_6H_3)_2CH\}]$ (**2**). Anisotropic displacement parameters are depicted at the 50% probability level. C–H hydrogen atoms are omitted for clarity except for the one at the bridging CH group. Structural data are given in Tables 1–3.

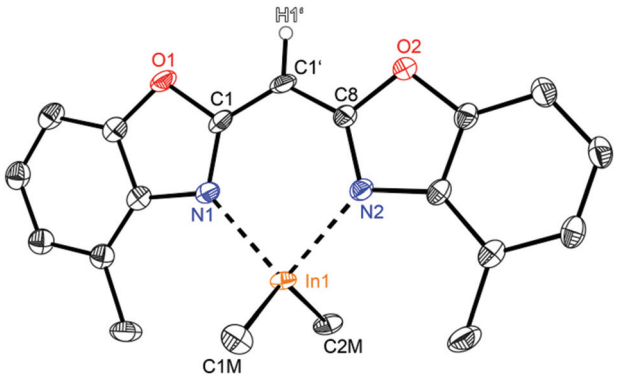

Fig. 5 Molecular structure of one molecule of $[Me_2In\{(4\text{-}MeN\text{-}COC_6H_3)_2CH\}]$ (**4**). Anisotropic displacement parameters are depicted at the 50% probability level. C–H hydrogen atoms are omitted for clarity except for the one at the bridging CH group. Structural data are given in Tables 1–3.

Compounds **2** (Fig. 3) and **3** (Fig. 4) are equi-structural and crystallise each in the monoclinic space group $P2_1/c$ and the asymmetric unit contains one molecule. **4** (Fig. 5) crystallises in the monoclinic space group *Pn* and contains two metallated molecules in the asymmetric unit (Table 4).

The structural comparison of the MMe_2 derivatives shows that in each case the metal coordination again is accomplished by the two nitrogen atoms of the benzoxazole moieties and the oxygen atoms are pointing away from the metal (Fig. 3–5). In all three cases this leads to a distorted tetrahedral coordination geometry at the particular metal ion. As expected the ligand framework in **2–4** exhibits nearly no folding of the heterocyclic residues. Additionally the metal ion is located in the C_3N_2 plane of the central six-membered metalla heterocycle without any significant deviation (see Table 2). Only this arrangement facilitates total conjugation of the whole anionic ligand. Due to the fourfold coordination of the metal ion the methyl residues at that metal are aligned perpendicularly with respect to the N1–M–N2 plane. This V-shaped arrangement of the MMe_2 fragments allows the organometallic fragment to slot in between the methyl groups of the ligand. The four methyl groups frame the group 13 metal to stay in plane (see Fig. 6).

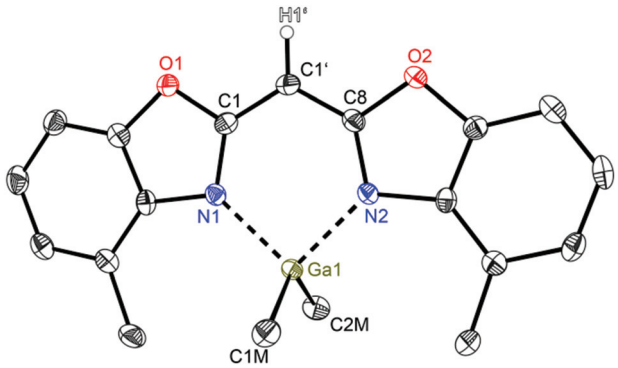

Fig. 4 Molecular structure of $[Me_2Ga\{(4\text{-}MeNCO\ C_6H_3)_2CH\}]$ (**3**). Anisotropic displacement parameters are depicted at the 50% probability level. C–H hydrogen atoms are omitted for clarity except for the one at the bridging CH group. Structural data are given in Tables 1–3.

Table 2 Selected folding parameters for compounds **1–7**

	Folding angle [°]	M-plane distance [Å]
1	—	—
2	3.721(20)	0.0054(22)
3	3.803(20)	0.0068(23)
4[a]	4.925(122)	0.0572(287)
	6.225(263)	0.1545(269)
5	3.394(20)	0.0090(19)
6	3.042(16)	0.0226(37)
7	4.425(71)	0.0483(20)

[a] Two values are given due to the discrepancy of the two molecules within the unit cell.

In the row of the investigated group 13 metal complexes **2–4** of the bis-(4-methylbenzoxazol-2-yl)-methanide ligand some clear trends from the obtained structural data could be deduced (see Table 3):

- The transannular N1···N2 distance, which is indicative of the size of the chelated metal atom, increases from **2** over **3** to **4** as expected, because the bigger the coordinated ion, the wider the chelating distance.
- Also the observed N–M distances increase according to the increasing ionic radii of the Al^{3+}, Ga^{3+} or In^{3+} ion, respectively.
- As a further consequence of this bond elongation and due to the fact that the metal stays in the ligand plane the resulting N1–M–N2 bite angles decrease from **2** over **3** to **4**.

In Fig. 6 compound **2** is exemplarily compared to the literature known nacnac derivatives $[Me_2Al\{Dipp_2nacnac\}]$[13i] (**A**) and $[Al\{Dipp_2nacnac\}]$[14e] (**B**) containing also the Al(III)Me_2 or Al(I) moiety, respectively. From the space filling model the steric

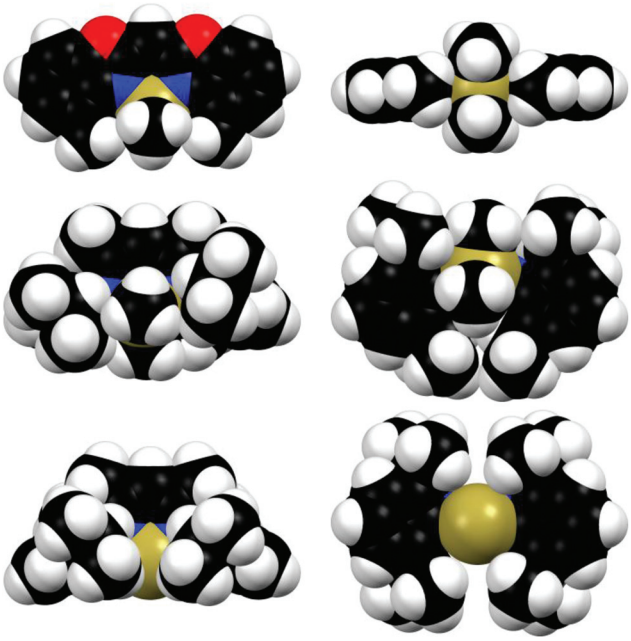

Fig. 6 Space filling models from different perspectives (left column: front view, right column: bottom view) of the compared aluminium complexes **2** (top), [$Me_2Al\{Dipp_2nacnac\}$][13i] (**A**) (middle) and [$Al\{Dipp_2$-nacnac$\}$][14e] (**B**) (bottom).

Table 3 Selected averaged bond lengths (Å) and angles (°) for compounds **1–7**

	N1···N2	N1/2–M	C15/16···M	N1–M–N2
1	3.5448(18)	—	—	—
2	2.8534(19)	1.9400(14)	3.4478(19)	94.68(6)
3	2.9010(23)	2.0043(15)	3.4474(22)	92.73(6)
4	3.0485(55)	2.217(9)	3.4805(167)	86.89(14)
5	2.8500(20)	1.9097(14)	3.4736(19)	96.52(6)
6	2.8775(37)	1.909(2)	3.5380(25)	97.84(12)
7	2.8753(21)	1.9140(16)	3.5341(22)	97.38(7)
A	2.870(4)	1.929(2)	3.789(3)	96.18(9)
B	2.764(3)	1.958(2)	3.606(3)	89.86(8)

demand of each ligand can be visualised and provides a fair estimate of the shielding abilities around the metal atoms.

Starting with the crystal structure of the Al(I) species **B** it is evident that the metal atom is located almost ideally within the chelating C_3N_2 plane (Fig. 6, bottom). The *N*,*N*′-coordinated metal atom fits well into the pocket made up of the four iPr groups of the Dipp substituents and the carbon atoms in the *ortho*-position of the associated phenyl rings. Furthermore, these phenyl rings are nearly perpendicularly aligned with respect to the C_3N_2 plane (89° and 91°). The *ortho*-carbon atoms provide the closest contact to the aluminium atom (averaged 3.606 Å) and presumably are equally important for the shielding of low-valent Al(I) species (listed in column C15/16···M in Table 3), because these distances are located between the nacnac species and the complexes derived from **1**. The bottom view also shows that the aluminium atom is not exhaustively coordinated so that coordination of the Lewis acidic site is facilitated. The side view highlights the good shielding abilities of the iPr groups, preventing the molecule from aggregation.

Continuing with the dimethyl aluminium species **A** the crystal structure clearly deviates from the reduced species **B**. The central six-membered metalla heterocycle is less planar than in **B**, because the $AlMe_2$ unit is not located in the chelating C_3N_2 plane. Furthermore, one of the two phenyl rings of the Dipp-substituents is considerably twisted away from orthogonality with respect to the C_3N_2 plane (112°). This deviation is caused by the additional methyl groups at the aluminium, which increases the steric demand compared to the naked metal in **B**. The formed pocket in **B** is not appropriate in size to accommodate the additional methyl groups. Instead of retaining the perpendicular alignment of the Dipp-substituents one of them is pushed away.

As mentioned earlier the methyl substituents of the chelating ligand in **2** adopt the shielding role of the Dipp residues of the comparable nacnac complexes. These efficient shielding abilities are visualised in the space filling model in the bottom view of **2** in Fig. 6: by chelation of the two nitrogen donor atoms of the ligand the $AlMe_2$ fragment is aligned in the C_3N_2 plane without any significant deviation. This planarity is also supported by the ligand's methyl groups, which fit nearly perfectly into the pocket made up of the V-shaped coordinated $AlMe_2$ cation. So in comparison with **A** and **B** the kinetic shielding considered from the bottom view is even more pronounced. As opposed to this the side view of **2** shows that the planar arrangement of the complex leads to less steric congestion from this point of view. The shielding abilities in **2** are not that encompassing as in the case of **A** and **B**, so that beneficial, specific substitution reactions at the metal centre still can take place. This advantageous property is exploited by the synthesis of **5** described in the following paragraph.

Structural comparison of 5–7

In addition to the dimethyl substituted group 13 metal complexes **2–4** three Al(III) derivatives, in which one of the methyl groups is replaced by a halide, were successfully synthesised as well. This substitution is necessary to improve the reactivity of those species compared to the relatively high stability of the dimethyl aluminium complexes. These reaction products should facilitate access to Al(I) or Al(II) species upon reductive dehalogenation reactions.

The synthesis of compounds **5** and **7** parallels the procedures of the abovementioned dimethyl derivatives. To a solution of the parent ligand **1** in toluene the pure organometallic reagent $AlMe_2Cl$ or $AlEt_2I$, respectively, was added in a slight excess at 0 °C (Scheme 3, pathway a). Differently **6** was prepared starting from the metallated species **2** by reaction with an excess of trimethyl silyl iodide to prompt a methyl iodide exchange at the metal atom (Scheme 3, pathway b).

Having a closer look at the geometrical data of those halide substituted species **5–7** the following conclusions can be

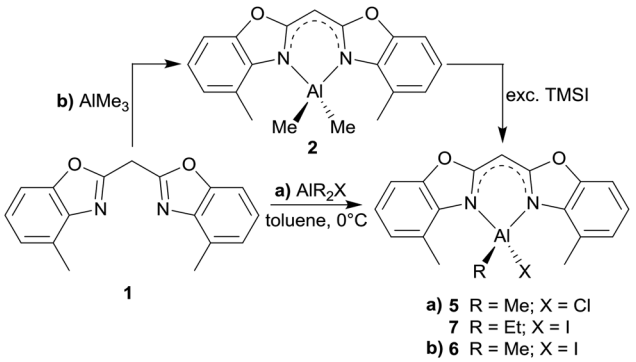

Scheme 3 Synthesis route for the mono halide substituted aluminium complexes **5–7**.

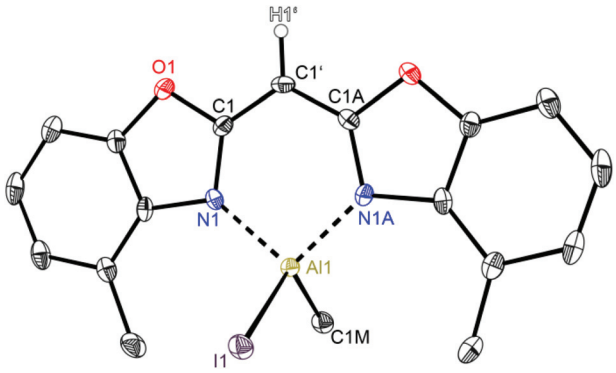

Fig. 8 Molecular structure of [IMeAl{(4-MeNCOC$_6$H$_3$)$_2$ CH}] (**6**). Anisotropic displacement parameters are depicted at the 50% probability level. C–H hydrogen atoms are omitted for clarity except for the one at the bridging CH group. Structural data are given in Tables 1–3.

made: the derivatives **5** (Fig. 7) and **7** (Fig. 9) crystallise in the monoclinic space group $P2_1/c$ each and the asymmetric unit consists in both cases of one target molecule. Compound **6** (Fig. 8) crystallises in the orthorhombic space group *Pbcm* and the asymmetric unit contains half a molecule (Table 4).

In the halogenated complexes the aluminium atom adopts also the distorted tetrahedral coordination by means of the two nitrogen donors and the remaining substituents at the metal atom. In direct comparison with the $AlMe_2$ derivative **2** the N–Al distances in **5–7** are increased and consequentially the corresponding N–Al–N bite angle is widened (see Table 3). These observed changes are caused by the electron withdrawing halide ligands Cl or I. These substituents increase the partial positive charge at the metal atom due to the negative inductive effect and their reduced electronegativity compared to carbon. The substituted aluminium atom needs less electron density from the donating nitrogen ring atoms and the nitrogen Lewis donors are less attractive.

The influence of the present halide atom on specific binding properties is displayed in Table 3. **5** compared to **6** shows the bigger halide iodide to cause the transannular N1···N2 distance to increase by about 0.03 Å (2.8500 Å in **5** *vs.* 2.8775 Å in **6**). This widening of the coordination pocket is also displayed in the bite angle, which also gets enlarged from 96.52° to 97.84°. Predominantly the higher steric demand of the iodide compared to the chloride accounts for the structural changes in the ligand. The observed differences among the two iodide derivatives **6** and **7** concerning those values are negligible. Within the triple estimated standard deviations the values for both species are the same, indicating that the slightly enhanced steric demand in **7** due to the ethyl group instead of a methyl group has no significant effect on those structural features.

Conclusions

In this work the successful syntheses and solid state structure determination of six metallated bis-(4-methylbenzoxazol-2-yl)-methanides **2–7** and the parent uncharged methane derivative **1** could be presented. As a consequence of tuning the pre-

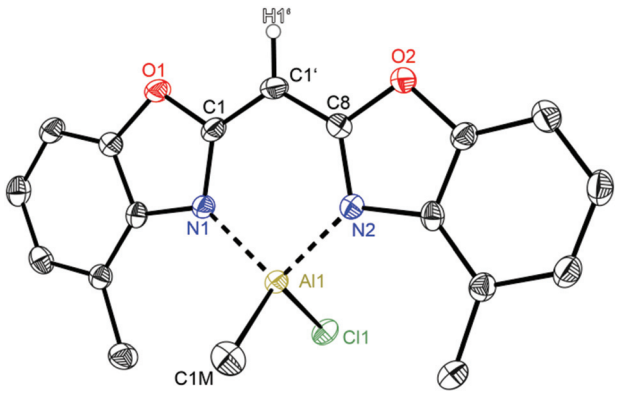

Fig. 7 Molecular structure of [ClMeAl{(4-MeNCOC$_6$H$_3$)$_2$ CH}] (**5**). Anisotropic displacement parameters are depicted at the 50% probability level. C–H hydrogen atoms are omitted for clarity except for the one at the bridging CH group. Structural data are given in Tables 1–3.

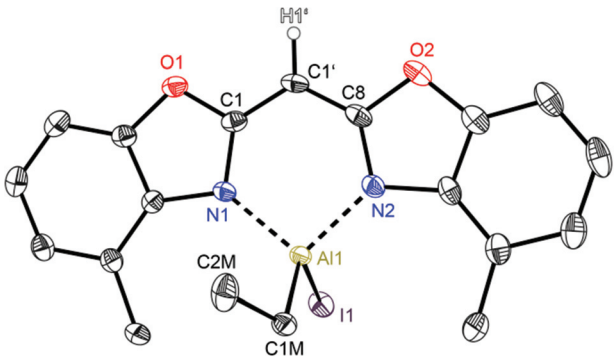

Fig. 9 Molecular structure of [IEtAl{(4-MeNCOC$_6$H$_3$)$_2$ CH}] (**7**). Anisotropic displacement parameters are depicted at the 50% probability level. C–H hydrogen atoms are omitted for clarity except for the one at the bridging CH group. Structural data are given in Tables 1–3.

Table 4 Crystal structure data for **1–7**

	1	**2**	**3**	**4**	**5**	**6**	**7**
Formula	$C_{17}H_{14}N_2O_2$	$C_{19}H_{19}AlN_2O_2$	$C_{19}H_{19}GaN_2O_2$	$C_{19}H_{19}InN_2O_2$	$C_{18.1}H_{16.3}AlCl_{0.9}N_2O_2$	$C_{18}H_{16}AlIN_2O_2$	$C_{19}H_{18}AlIN_2O_2$
Mol. w., g mol^{-1}	278.31	334.35	377.10	422.18	352.59	446.21	460.23
CCDC no.	1429338	1429357	1429403	1429339	1429341	1429342	1429343
Wavelength, Å	0.71073	0.71073	0.56086	0.56086	0.56086	0.56086	0.71073
Crystal system	Triclinic	Monoclinic	Monoclinic	Monoclinic	Monoclinic	Orthorhombic	Monoclinic
Space group	$P\bar{1}$	$P2_1/c$	$P2_1/c$	Pn	$P2_1/c$	$Pbcm$	$P2_1/c$
a, Å	4.741(2)	8.029(2)	7.986(2)	15.629(3)	7.982(2)	8.015(2)	9.102(3)
b, Å	11.471(3)	14.773(3)	14.852(3)	7.894(2)	14.727(3)	13.868(3)	7.647(2)
c, Å	13.084(3)	14.072(3)	14.087(3)	15.631(3)	13.890(2)	15.566(3)	26.711(4)
α, °	79.15(2)	90	90	90	90	90	90
β, °	85.84(2)	90.03(2)	90.12(2)	117.04(2)	91.73(2)	90	96.59(2)
γ, °	78.19(2)	90	90	90	90	90	90
V, Å^3	683.6(4)	1669.1(6)	1670.81(9)	1717.7(7)	1632.0(6)	1730.2(6)	1846.9(8)
Z	2	4	4	4	4	4	4
Refl. measured	23 615	57 930	45 271	49 033	20 579	25 400	38 660
Refl. unique	2495	3060	3069	8534	2904	1915	4398
R_1 $[I > 2\sigma(I)]$[a]	0.0364	0.0306	0.0248	0.0248	0.0322	0.0222	0.0210
wR_2 (all refl.)[b]	0.0938	0.0868	0.0672	0.0546	0.0885	0.0542	0.0534
R_{int}	0.0369	0.0384	0.0445	0.0481	0.0370	0.0431	0.0231
Abs. stru. para.[26]	—	—	—	0.11(4)	—	—	—
$\Delta\rho_{fin}$, e Å^{-3}	0.170/−0.162	0.222/−0.323	0.386/−0.372	0.334/−0.463	0.206/−0.314	0.502/−0.894	0.730/−0.406

[a] $R_1 = \frac{\sum |F_o| - |F_c|}{\sum |F_o|}$. [b] $wR_2 = \frac{\sum w(F_o^2 - F_c^2)^2}{\sum (w(F_o^2)^2}$; $w = \frac{1}{\sigma^2(F_o^2) + (g_1P)^2 + g_2P}$; $P = \frac{(F_o^2 + 2F_c^2)}{3}$.

viously reported bisheterocyclo methanes by introducing methyl groups to the benzannulated heterocycles (in this case benzoxazole) a promising ligand system for metal complexation could be obtained, which exhibits a nearly perfect planar coordination geometry with regard to the ligand side arms in all the discussed solid state structures. This fact is displayed by the small values in the folding angles between both heteroaromatic planes and the just slight deviations of the metal cations from the chelating C_3N_2 plane in each complex, which is outstanding in the row of the previously investigated methanide and amide complexes. The observed arrangement in the solid state can be explained by the steric strain induced by the additional methyl groups, which fit inside the properly shaped pocket made up the particular V-shaped MR_2 fragments, so that a kind of intramolecular interlocking is responsible for the overall planar arrangement.

Due to the relatively pronounced inertness of the dimethyl group 13 metal complexes the switch to the mono halide substituted compounds **5–7** offers access to low-valent group 13 complexes, which hopefully can be obtained by reductive salt elimination analogous to the synthesis route of [Al{Dipp$_2$-nacnac}] or [Ga{Dipp$_2$nacnac}]. The steric protection around the metal centre resulting from the planar organic ligand is quite efficient for kinetic stabilisation, but in the case of **2** the reaction with an excess of trimethyl silyl iodide showed that specific substitution reactions can still take place, which is beneficial in contrast to the former nacnac derivatives. Nevertheless, it is worth mentioning, that even an excess of TMSI does not lead to a dual halide substituted derivative. Because of the beneficial planar arrangement of the ligand system and the metal cation within the precursors **2**, and **5–7** the generation of new Al(I) species is feasible. The planar coordination geometry should enable optimal orbital overlapping between the endocyclic nitrogen donors and the chelated future low-valent metal atom to obtain a more efficient delocalisation. Further substitution and reduction attempts on aluminium containing complexes of this promising ligand system are under investigation.

Experimental section

General procedures

All manipulations were carried out under an atmosphere of dried and purified N_2 or Ar by using Schlenk techniques.[24] All solvents used within metallation reactions were distilled from Na or K prior to use. The starting materials were purchased commercially and used as received. ^{1}H, ^{13}C, ^{15}N and ^{27}Al NMR spectroscopic data were recorded on Bruker Avance 500 MHz, Bruker Avance 400 MHz and Bruker Avance 300 MHz spectrometers and referenced to the deuterated solvent (thf-d$_8$).[25] Elemental analyses (C, H, N and S) were carried out on a Vario EL3 at the Mikroanalytisches Labor, Institut für Anorganische Chemie, University of Göttingen. All EI-MS spectra (70 eV) were recorded on a Finnigan MAT 95.

(4-MeNCOC$_6$H$_3$)$_2$CH$_2$ (1). *Method 1*: 2-Amino-3-methylphenol (2.91 g, 23.6 mmol, 2.00 eq.) and ethylbisimidate dihydrochloride (2.73 g, 11.8 mmol, 1.00 eq.) were dissolved in methanol (55 mL). The heating time of the reaction mixture was extended for reflux overnight and after cooling to rt stored at −32 °C in a refrigerator. The resulting crystalline material was filtered off, washed with saturated aqueous $NaHCO_3$ solution (3 × 50 mL) and water (3 × 50 mL) and dried under reduced pressure. Crystals suitable for X-ray diffraction experi-

ments could be obtained upon recrystallisation from toluene. Pale brown crystals were obtained in a yield of 1.43 g (5.15 mmol, 44%).

Method 2: A mixture of 2-amino-3-methylphenol (9.85 g, 80.0 mmol, 2.00 eq.) and malonic acid (4.16 g, 40.0 mmol, 1.00 eq.) was suspended in polyphosphoric acid (100 mL) with the use of a sealed precision glass (KPG) stirrer. Under vigorous stirring the reaction mixture was heated to 150 °C and the resulting dark blue viscous solution was kept under stirring at this elevated temperature for 5 h. Then the solution was allowed to cool to about 90 °C and poured over ice. The formed grey solid was filtered off, washed several times with saturated aqueous $NaHCO_3$ solution (9 × 50 mL) and distilled water (10 × 50 mL) to pH neutrality. The remaining solvent was evaporated *in vacuo* to obtain **1** (6.26 g, 22.5 mmol, 56%) as a pale grey powder.

Anal. Calcd for $C_{17}H_{14}N_2O_2$ (278.31 g mol^{-1}): C, 73.37; H, 5.07; N, 10.07. Found: C, 72.90; H, 5.14; N, 9.90; δ^1H (300 MHz, thf-d$_8$): 7.33 (d, $^3J_{HH}$ = 8.1 Hz, 2 H, H3), 7.20 (t, $^3J_{HH}$ = 7.8 Hz, 2 H, H4), 7.11 (d, $^3J_{HH}$ = 7.5 Hz, 2 H, H5), 4.68 (s, 2 H, H1′), 2.55 (s, 6 H, H15); δ^{13}C{^{1}H} (75 MHz, thf-d$_8$): 160.62 (s, 2 C, C1), 152.05 (s, 2 C, C2), 141.74 (s, 2 C, C7), 131.32 (s, 2 C, C6), 125.62 (s, 2 C, C4), 125.58 (s, 2 C, C5), 108.58 (s, 2 C, C3), 29.69 (s, 1 C, C1′), 16.41 (s, 2 C, C15); δ^{15}N{^{1}H} (30 MHz, thf-d$_8$): −135.9 (s); EI-MS, *m*/*z* (%): 278 (100) [M]$^+$, 146 (10) [M − NCOC$_7$H$_6$]$^+$.

Metallation reactions

To a solution of the corresponding ligand **1** (1.00 eq.) in toluene a slight excess of the pure organometallic reactant $AlMe_3$, $GaMe_3$, $InMe_3$, $AlMe_2Cl$ or $AlEt_2I$, respectively (1.10 eq.) was slowly added at 0 °C. The reaction mixture was stirred overnight and allowed to warm to rt. Afterwards the volume of the solution was reduced to a few mL and the resulting concentrated solution stored at −32 °C in a refrigerator. Crystals suitable for X-ray diffraction experiments could be obtained overnight. The crystals thus formed were filtered, washed twice with pre-cooled toluene or hexane (0 °C) and finally dried in vacuum. The given yields below are just based on the received crystals unless stated otherwise. No further improvement of the yields was attempted.

[Me$_2$Al{(4-MeNCOC$_6$H$_3$)$_2$CH}] (2). 1 (4.66 g, 16.7 mmol, 1.00 eq.) dissolved in toluene (120 mL) and trimethyl aluminium (1.80 mL, 1.33 g, 18.4 mmol, 1.10 eq.) were treated as stated in the general procedure above. Yellow crystals were obtained in a yield of 3.79 g (11.3 mmol, 68%). Anal. Calcd for $C_{19}H_{19}AlN_2O_2$ (334.35 g mol^{-1}): C, 68.25; H, 5.73; N, 8.38. Found: C, 68.21; H, 6.18; N, 8.30; δ^1H (500 MHz, thf-d$_8$): 7.26–7.22 (m, 2 H, H3), 7.11–7.06 (m, 4 H, H4 + H5), 5.33 (s, 1 H, H1′), 2.66 (s, 6 H, H15), −0.38 (s, 6 H, H1M); δ^{13}C{^{1}H} (125 MHz, thf-d$_8$): 168.70 (s, 2 C, C1), 149.29 (s, 2 C, C2), 136.98 (s, 2 C, C7), 127.63 (s, 2 C, C5), 124.33 (s, 2 C, C6), 123.81 (s, 2 C, C4), 108.01 (s, 2 C, C3), 59.95 (s, 1 C, C1′), 19.51 (s, 2 C, C15), −3.86 (s, 2 C, C1M); δ^{15}N{^{1}H} (50 MHz, thf-d$_8$): −230.5 (s); δ^{27}Al{^{1}H} (130 MHz, thf-d$_8$): 153 (s); EI-MS, *m*/*z* (%): 334.1 (10) [M]$^+$, 319.1 (64) [M − Me]$^+$, 303.1 (5) [M − 2 Me]$^+$, 278.1 (100) [M − AlMe$_2$]$^+$.

[Me$_2$Ga{(4-MeNCOC$_6$H$_3$)$_2$CH}] (3). 1 (1.39 g, 5.00 mmol, 1.00 eq.) dissolved in toluene (25 mL) and trimethyl gallium (0.56 mL, 632 mg, 5.50 mmol, 1.10 eq.) were treated as stated in the general procedure above. Brownish yellow crystals were obtained in a yield of 308 mg (0.82 mmol, 17%; not optimised). Anal. Calcd for $C_{19}H_{19}GaN_2O_2$ (377.10 g mol^{-1}): C, 60.52; H, 5.08; N, 7.43. Found: C, 60.84; H, 5.24; N, 7.45; δ^1H (400 MHz, thf-d$_8$): 7.22–7.13 (m, 2 H, H3), 7.07–6.99 (m, 4 H, H4 + H5), 5.18 (s, 1 H, H1′), 2.57 (s, 6 H, H15), 0.06 (s, 6 H, H1M); δ^{13}C{^{1}H} (75 MHz, thf-d$_8$): 167.84 (s, 2 C, C1), 149.20 (s, 2 C, C2), 137.57 (s, 2 C, C7), 127.27 (s, 2 C, C5), 123.60 (s, 2 C, C6), 123.15 (s, 2 C, C4), 107.85 (s, 2 C, C3), 58.83 (s, 1 C, C1′), 19.01 (s, 2 C, C15), −0.95 (s, 2 C, C1M); δ^{15}N{^{1}H} (40 MHz, thf-d$_8$): −229.7 (s); EI-MS, *m*/*z* (%): 376.1 (17) [M]$^+$, 361.0 (100) [M − Me]$^+$, 346.0 (20) [M − 2 Me]$^+$, 277.1 (12) [M − GaMe$_2$]$^+$, 68.9 (41) Ga$^+$.

[Me$_2$In{(4-MeNCOC$_6$H$_3$)$_2$CH}] (4). 1 (278 mg, 1.00 mmol, 1.00 eq.) dissolved in toluene (60 mL) and trimethyl indium (0.30 mL) were treated as stated in the general procedure above. Because the used $InMe_3$ solution had an unknown concentration, no further statements regarding the equivalents or yield can be made. Orange crystals were obtained in a yield of 78 mg (0.18 mmol). Anal. Calcd for $C_{19}H_{19}InN_2O_2$ (422.18 g mol^{-1}): C, 54.05; H, 4.54; N, 6.64. Found: C, 54.52; H, 4.92; N, 6.70; δ^1H (500 MHz, thf-d$_8$): 7.18–7.13 (m, 2 H, H3), 7.00–6.95 (m, 4 H, H4 + H5), 5.12 (s, 1 H, H1′), 2.54 (s, 6 H, H15), 0.13 (s, 6 H, H1M); δ^{13}C{^{1}H} (125 MHz, thf-d$_8$): 168.36 (s, 2 C, C1), 148.95 (s, 2 C, C2), 139.27 (s, 2 C, C7), 126.58 (s, 2 C, C5), 122.94 (s, 2 C, C6), 122.66 (s, 2 C, C4), 107.81 (s, 2 C, C3), 59.07 (s, 1 C, C1′), 18.59 (s, 2 C, C15), −2.91 (s, 2 C, C1M); δ^{15}N{^{1}H} (50 MHz, thf-d$_8$): −226.2 (s).

[ClMeAl{(4-MeNCOC$_6$H$_3$)$_2$CH}] (5). 1 (1.39 g, 5.00 mmol, 1.00 eq.) dissolved in toluene (35 mL) and dimethyl aluminium chloride (0.51 mL, 509 mg, 5.50 mmol, 1.10 eq.) were treated as stated in the general procedure above. A pale yellow powder was obtained in a yield of 1.37 g (3.9 mmol, 77%). Anal. Calcd for $C_{18}H_{16}AlClN_2O_2$ (354.77 g mol^{-1}): C, 60.94; H, 4.55; N, 7.90. Found: C, 60.99; H, 4.57; N, 8.17; δ^1H (400 MHz, thf-d$_8$): 7.33–7.27 (m, 2 H, H3), 7.17–7.11 (m, 4 H, H4 + H5), 5.55 (s, 1 H, H1′), 2.78 (s, 6 H, H15), −0.14 (s, 3 H, H1M); δ^{13}C{^{1}H} (125 MHz, thf-d$_8$): 168.67 (s, 2 C, C1), 149.14 (s, 2 C, C2), 136.07 (s, 2 C, C7), 128.02 (s, 2 C, C5), 125.05 (s, 2 C, C6), 124.54 (s, 2 C, C4), 108.24 (s, 2 C, C3), 61.18 (s, 1 C, C1′), 19.93 (s, 2 C, C15), −3.68 (s, 1 C, C1M); δ^{15}N{^{1}H} (50 MHz, thf-d$_8$): −246.9 (s); δ^{27}Al{^{1}H} (78 MHz, thf-d$_8$): 128 (s); EI-MS, *m*/*z* (%): 278 (100) [M − AlMeCl]$^+$, 146 (45) [M − AlMeCl − NCOC$_7$H$_6$]$^+$, 132 (8) [NCOC$_7$H$_6$]$^+$.

[IMeAl{(4-MeNCOC$_6$H$_3$)$_2$CH}] (6). To a solution of **2** (334 mg, 1.00 mmol, 1.00 eq.) in toluene (20 mL) was added trimethylsilyl iodide (0.31 mL, 440 mg, 2.20 mmol, 2.20 eq.). The reaction mixture was heated to reflux temperature and stirred for an additional 3.5 d at reflux. The formed precipitate was filtered off and the residual solvent was removed under reduced pressure. The mono iodide substituted derivative

could be isolated as a brown powder (111 mg, 0.25 mmol, 25%). After recrystallization from toluene also crystals suitable for structure determination were obtained. Calcd for $C_{18}H_{16}AlIN_2O_2$ (446.22 g mol^{-1}): C, 48.45; H, 3.61; N, 6.28. Found: C, 45.53; H, 3.32; N, 6.07 (deviation due to slight contamination with the AlI_2 derivative); δ^1H (300 MHz, thf-d$_8$): 7.29–7.25 (m, 2 H, H3), 7.14–7.10 (m, 4 H, H4 + H5), 5.47 (s, 1 H, H1′), 2.77 (s, 6 H, H15), −0.47 (s, 3 H, H1M); δ^{13}C{^{1}H} (125 MHz, thf-d$_8$): 168.90 (s, 2 C, C1), 149.13 (s, 2 C, C2), 136.66 (s, 2 C, C7), 127.72 (s, 2 C, C5), 125.12 (s, 2 C, C6), 124.11 (s, 2 C, C4), 108.05 (s, 2 C, C3), 60.58 (s, 1 C, C1′), 18.88 (s, 2 C, C15), −6.83 (s, 1 C, C1M); δ^{15}N{^{1}H} (50 MHz, thf-d$_8$): −230.8 (s); EI-MS, *m*/*z* (%): 278 (100) [M − AlMeI]$^+$, 146 (37) [M − AlMeI − NCOC$_7$H$_6$]$^+$, 132 (9) [NCOC$_7$H$_6$]$^+$.

[IEtAl{(4-MeNCOC$_6$H$_3$)$_2$CH}] (7). To a solution of **1** (1.39 g, 5.00 mmol, 1.00 eq.) dissolved in toluene (80 mL) and diethylaluminium iodide (0.73 mL, 1.17 g, 5.50 mmol, 1.10 eq.) were treated as stated in the general procedure above. Orange crystals were obtained in a yield of 1.16 g (2.52 mmol, 50%; not optimised). Calcd for $C_{19}H_{18}AlIN_2O_2$ (460.24 g mol^{-1}): C, 49.58; H, 3.94; N, 6.09. Found: C, 49.35; H, 4.02; N, 6.09; δ^1H (400 MHz, thf-d$_8$): 7.29–7.24 (m, 2 H, H3), 7.14–7.11 (m, 4 H, H4 + H5), 5.46 (s, 1 H, H1′), 2.79 (s, 6 H, H15), 0.85 (t, $^3J_{HH}$ = 8.2 Hz, 3 H, H2M), 0.21 (q, $^3J_{HH}$ = 8.2 Hz, 2 H, H1M); δ^{13}C{^{1}H} (75 MHz, thf-d$_8$): 169.09 (s, 2 C, C1), 149.12 (s, 2 C, C2), 136.72 (s, 2 C, C7), 127.73 (s, 2 C, C5), 125.15 (s, 2 C, C6), 124.10 (s, 2 C, C4), 108.05 (s, 2 C, C3), 60.52 (s, 1 C, C1′), 18.74 (s, 2 C, C15), 8.66 (s, 1 C, C2M), 3.13 (s, 1 C, C1M); δ^{15}N{^{1}H} (40 MHz, thf-d$_8$): −232.3 (s); EI-MS, *m*/*z* (%): 278 (100) [M − AlEtI]$^+$, 146 (41) [M − AlEtI − NCOC$_7$H$_6$]$^+$, 132 (7) [NCOC$_7$H$_6$]$^+$.

X-ray crystallographic studies

Single crystals were selected from a Schlenk flask under an argon or a nitrogen atmosphere and covered with perfluorinated polyether oil on a microscope slide, which was cooled with a nitrogen gas flow using an X-TEMP2 device.[27] An appropriate crystal was selected using a polarised microscope, mounted on the tip of a MiTeGen©MicroMount or glass fibre, fixed to a goniometer head and shock cooled by a crystal cooling device. The data for **1–7** were collected from shock-cooled crystals at 100(2) K. The data of **1**, **2** and **7** were collected on an Incoatec Mo Microsource[28] and compounds **3–6** were collected on an Incoatec Ag Microsource,[29] each equipped with mirror optics and an APEX II detector with a D8 goniometer. All diffractometers were equipped with a low-temperature device and used either MoK$_\alpha$ radiation of λ = 0.71073 Å or AgK$_\alpha$ radiation of λ = 0.56086 Å. The data were integrated with Saint[30] and an semi-empirical absorption correction (Sadabs)[29] was applied. The structures were solved by direct methods (Shelxt)[31] and refined by full-matrix least-squares methods against F^2 (Shelxl2014).[32] All non-hydrogen-atoms were refined with anisotropic displacement parameters. The hydrogen atoms were refined isotropically on calculated positions using a riding model with their U_{iso} values constrained to equal 1.5 times the U_{eq} of their pivot atoms for terminal sp^3 carbon atoms and 1.2 times for all other carbon atoms. Disordered moieties were refined using bond length restraints and isotropic displacement parameter restraints. The positions of the amine hydrogen atoms are taken from the difference Fourier map and refined freely.

Crystallographic data for the structures reported in this paper have been deposited with the Cambridge Crystallographic Data Centre. The CCDC numbers, crystal data and experimental details for the X-ray measurements are listed in the ESI.‡

Conflict of interest

The authors declare no competing financial interest.

Acknowledgements

Thanks to the Danish National Research Foundation (DNRF93) funded Center for Materials Crystallography (CMC) for partial support and the Land Niedersachsen for providing a fellowship in the GAUSS PhD program.

Notes and references

1 P. P. Power, *Nature*, 2010, **463**, 171–177.
2 (*a*) D. W. Stephan, *Org. Biomol. Chem.*, 2008, **6**, 1535–1539; (*b*) W. Tochtermann, *Angew. Chem.*, 1966, **7**, 355–375, (*Angew. Chem. Int. Ed. Engl.*, 1966, **5**, 351–371); (*c*) G. Wittig and E. Benz, *Chem. Ber.*, 1959, **92**, 1999–2013.
3 (*a*) D. W. Stephan and G. Erker, *Angew. Chem.*, 2010, **122**, 50–81, (*Angew. Chem. Int. Ed.*, 2010, **49**, 46–76); (*b*) P. Spies, G. Kehr, K. Bergander, B. Wibbeling, R. Fröhlich and G. Erker, *Dalton Trans.*, 2009, 1534–1541; (*c*) G. C. Welch, R. R. S. Juan, J. D. Masuda and D. W. Stephan, *Science*, 2006, **314**, 1124–1126.
4 G. C. Welch, J. D. Masuda and D. W. Stephan, *Inorg. Chem.*, 2006, **45**, 478–480.
5 C. Appelt, J. C. Slootweg, K. Lammertsma and W. Uhl, *Angew. Chem.*, 2013, **52**, 4256–4259, (*Angew. Chem., Int. Ed.*, 2013, **52**, 4256–4259).
6 Y. Zhang, G. M. Miyake and E. Y. X. Chen, *Angew. Chem.*, 2010, **122**, 10356–10360, (*Angew. Chem. Int. Ed.*, 2010, **49**, 10158–10162).
7 (*a*) G. Ménard and D. W. Stephan, *Angew. Chem.*, 2011, **123**, 8546–8549, (*Angew. Chem. Int. Ed.*, 2011, **50**, 8396–8399); (*b*) G. Ménard and D. W. Stephan, *J. Am. Chem. Soc.*, 2010, **132**, 1796–1797.
8 L. Bourget-Merle, M. F. Lappert and J. R. Severn, *Chem. Rev.*, 2002, **102**, 3031–3065.
9 (*a*) J. Overgaard, C. Jones, A. Stasch and B. B. Iversen, *J. Am. Chem. Soc.*, 2009, **131**, 4208–4209; (*b*) M. Westerhausen, *Angew. Chem.*, 2008, **120**, 2215–2217, (*Angew. Chem. Int. Ed.*, 2008, **47**, 2185–2187); (*c*) S. P. Green, C. Jones and A. Stasch, *Science*, 2007, **318**, 1754–1757.

10 (*a*) C. Ruspic and S. Harder, *Inorg. Chem.*, 2007, **46**, 10426–10433; (*b*) S. Harder, *Organometallics*, 2002, **21**, 3782–3787.
11 D. F. J. Piesik, S. Range and S. Harder, *Organometallics*, 2008, **27**, 6178–6187.
12 J. Spielmann, F. Buch and S. Harder, *Angew. Chem.*, 2008, **120**, 9576–9580, (*Angew. Chem. Int. Ed.*, 2008, **47**, 9434–9438).
13 (*a*) Y. Cheng, D. J. Doyle, P. B. Hitchcock and M. F. Lappert, *Dalton Trans.*, 2006, 4449–4460; (*b*) S. Singh, H.-J. Ahn, A. Stasch, V. Jancik, H. W. Roesky, A. Pal, M. Biadene, R. Herbst-Irmer, M. Noltemeyer and H.-G. Schmidt, *Inorg. Chem.*, 2006, **45**, 1853–1860; (*c*) Z. Yang, H. Zhu, X. Ma, J. Chai, H. W. Roesky, C. He, J. Magull, H.-G. Schmidt and M. Noltemeyer, *Inorg. Chem.*, 2006, **45**, 1823–1827; (*d*) N. Kuhn, S. Fuchs and M. Steimann, *Z. Anorg. Allg. Chem.*, 2002, **628**, 458–462; (*e*) N. Kuhn, S. Fuchs and M. Steimann, *Eur. J. Inorg. Chem.*, 2001, **2001**, 359–361; (*f*) M. Stender, B. E. Eichler, N. J. Hardman, P. P. Power, J. Prust, M. Noltemeyer and H. W. Roesky, *Inorg. Chem.*, 2001, **40**, 2794–2799; (*g*) N. Kuhn, J. Fahl, S. Fuchs, M. Steimann, G. Henkel and A. H. Maulitz, *Z. Anorg. Allg. Chem.*, 1999, **625**, 2108–2114; (*h*) C. E. Radzewich, I. A. Guzei and R. F. Jordan, *J. Am. Chem. Soc.*, 1999, **121**, 8673–8674; (*i*) B. Qian, D. L. Ward and M. R. Smith, *Organometallics*, 1998, **17**, 3070–3076.
14 (*a*) S. Nagendran and H. W. Roesky, *Organometallics*, 2008, **27**, 457–492; (*b*) X. Li, X. Cheng, H. Song and C. Cui, *Organometallics*, 2007, **26**, 1039–1043; (*c*) H. W. Roesky and S. S. Kumar, *Chem. Commun.*, 2005, 4027–4038; (*d*) M. N. Sudheendra Rao, H. W. Roesky and G. Anantharaman, *J. Organomet. Chem.*, 2002, **646**, 4–14; (*e*) C. Cui, H. W. Roesky, H.-G. Schmidt, M. Noltemeyer, H. Hao and F. Cimpoesu, *Angew. Chem.*, 2000, **112**, 4444–4446, (*Angew. Chem. Int. Ed.*, 2000, **39**, 4274–4276).
15 N. J. Hardman, B. E. Eichler and P. P. Power, *Chem. Commun.*, 2000, 1991–1992.
16 (*a*) P. Hao, Z. Yang, W. Li, X. Ma, H. W. Roesky, Y. Yang and J. Li, *Organometallics*, 2015, **34**, 105–108; (*b*) B. Li, C. Zhang, Y. Yang, H. Zhu and H. W. Roesky, *Inorg. Chem.*, 2015, **54**, 6641–6646; (*c*) Z. Yang, M. Zhong, X. Ma, S. De, C. Anusha, P. Parameswaran and H. W. Roesky, *Angew. Chem.*, 2015, **127**, 10363–10367, (*Angew. Chem. Int. Ed.*, 2015, **54**, 10225–10229); (*d*) Y. Yang, H. Li, C. Wang and H. W. Roesky, *Inorg. Chem.*, 2012, **51**, 2204–2211.
17 (*a*) Z. Zhu, X. Wang, Y. Peng, H. Lei, J. C. Fettinger, E. Rivard and P. P. Power, *Angew. Chem.*, 2009, **121**, 2065–2068, (*Angew. Chem. Int. Ed.*, 2009, **48**, 2031–2034); (*b*) R. J. Wright, M. Brynda and P. P. Power, *Angew. Chem.*, 2006, **118**, 6099–6102, (*Angew. Chem. Int. Ed.*, 2006, **45**, 5953–5956); (*c*) R. J. Wright, A. D. Phillips, S. Hino and P. P. Power, *J. Am. Chem. Soc.*, 2005, **127**, 4794–4799; (*d*) N. J. Hardman, R. J. Wright, A. D. Phillips and P. P. Power, *Angew. Chem.*, 2002, **114**, 2966–2968, (*Angew. Chem. Int. Ed.*, 2002, **41**, 2842–2844); (*e*) J. Su, X.-W. Li, R. C. Crittendon and G. H. Robinson, *J. Am. Chem. Soc.*, 1997, **119**, 5471–5472.
18 D.-R. Dauer and D. Stalke, *Dalton Trans.*, 2014, **43**, 14432–14439.
19 D.-R. Dauer, M. Flügge, R. Herbst-Irmer and D. Stalke, *Dalton Trans.*, 2015, DOI: 10.1039/C5DT03911H.
20 (*a*) F. Baier, Z. Fei, H. Gornitzka, A. Murso, S. Neufeld, M. Pfeiffer, I. Rüdenauer, A. Steiner, T. Stey and D. Stalke, *J. Organomet. Chem.*, 2002, **661**, 111–127; (*b*) H. Gornitzka and D. Stalke, *Angew. Chem.*, 1994, **106**, 695–698, (*Angew. Chem. Int. Ed. Engl.*, 1994, **33**, 693–695); (*c*) H. Gornitzka and D. Stalke, *Organometallics*, 1994, **13**, 4398–4405.
21 W. W. Schoeller, *Inorg. Chem.*, 2011, **50**, 2629–2633.
22 H. Ben Ammar, J. Le Nôtre, M. Salem, M. T. Kaddachi and P. H. Dixneuf, *J. Organomet. Chem.*, 2002, **662**, 63–69.
23 (*a*) P. Müller, R. Herbst-Irmer, A. L. Spek, T. R. Schneider and M. R. Sawaya, *Crystal Structure Refinement A Crystallographer's Guide to SHELXL*, Oxford University Press, New York, 2006; (*b*) P. Rademacher, *Strukturen organischer Moleküle*, VCH, Weinheim, 1987.
24 Georg-August-Universität Göttingen, Virtuelles Labor, http://www.stalke.chemie.uni-goettingen.de/virtuelles_labor/advanced/13_de.html.
25 Georg-August-Universität Göttingen, Virtuelles Labor, http://www.stalke.chemie.uni-goettingen.de/virtuelles_labor/nmr/de.html.
26 S. Parsons, H. D. Flack and T. Wagner, *Acta Crystallogr., Sect. B: Struct. Sci.*, 2013, **69**, 249–259.
27 (*a*) D. Stalke, *Chem. Soc. Rev.*, 1998, **27**, 171–178; (*b*) T. Kottke, R. J. Lagow and D. Stalke, *J. Appl. Crystallogr.*, 1996, **29**, 465–468; (*c*) T. Kottke and D. Stalke, *J. Appl. Crystallogr.*, 1993, **26**, 615–619; (*d*) Georg-August-Universität Göttingen, Virtuelles Labor, http://www.stalke.chemie.uni-goettingen.de/virtuelles_labor/special/22_de.html.
28 T. Schulz, K. Meindl, D. Leusser, D. Stern, J. Graf, C. Michaelsen, M. Ruf, G. M. Sheldrick and D. Stalke, *J. Appl. Crystallogr.*, 2009, **42**, 885–891.
29 L. Krause, R. Herbst-Irmer, G. M. Sheldrick and D. Stalke, *J. Appl. Crystallogr.*, 2015, **48**, 3–10.
30 Bruker AXS Inc., in *Bruker Apex CCD, SAINT v8.30C*, ed. Bruker AXS Inst. Inc., WI, USA, Madison, 2013.
31 G. Sheldrick, *Acta Crystallogr., Sect. A: Fundam. Crystallogr.*, 2015, **71**, 3–8.
32 (*a*) G. Sheldrick, *Acta Crystallogr., Sect. C: Cryst. Struct. Commun.*, 2015, **71**, 3–8; (*b*) G. M. Sheldrick, *Acta Crystallogr., Sect. A: Fundam. Crystallogr.*, 2014, **70**, C1437; (*c*) G. M. Sheldrick, *Acta Crystallogr., Sect. A: Fundam. Crystallogr.*, 2008, **64**, 112–122.